



# Evolution of porous structure with dealloying corrosion on Gasar Cu–Mn alloy

Xing-ming ZHANG<sup>1</sup>, Yan-xiang LI<sup>1,2</sup>, Hua-wei ZHANG<sup>1,2</sup>, Yuan LIU<sup>1,2</sup>

1. School of Materials Science and Engineering, Tsinghua University, Beijing 100084, China;

2. Key Laboratory for Advanced Materials Processing Technology,  
Ministry of Education, Tsinghua University, Beijing 100084, China

Received 17 April 2014; accepted 13 July 2014

**Abstract:** The evolution of nanoporous structure with dealloying condition was investigated, thus, the mechanism of porous structure evolution was uncovered. The Gasar Cu–Mn alloy was dealloyed by room and elevated temperature chemical corrosion, low and high current level electrochemical corrosion, four types of porous structures, including uneven corrosion pits, hybrid porous, haystack type and bicontinuous model were prepared by chemically and electrochemically dealloying the porous Cu–34.6%Mn alloy made by the Gasar process. Then, the surface diffusion coefficient ( $D_S$ ) and the diffusion frequency ( $k_D$ ) of Cu atom, as well as the dissolution frequency ( $k_E$ ) of Mn atom were calculated with dealloying condition. The dealloyed morphologies for room temperature chemical corrosion and low current level electrochemical corrosion were similar due to the same  $D_S$ . While the dealloyed structures changed from bulk hybrid porous structure to bicontinuous porous film with decreasing  $k_D/k_E$ .

**Key words:** Gasar process; dealloying; hybrid porous; nanoporous structure

## 1 Introduction

Dealloying is a selective corrosion method usually applied to binary solid solution systems to fabricate nanoporous metals. During dealloying process, the active component dissolves, while the inactive component diffuses and rearranges to form a bicontinuous nanoporous structure [1]. NEWMAN et al [2] pointed out that dealloying was a competition between selective dissolution which roughened the surface and surface diffusion which smoothed the surface. ERLEBACHER et al [3] investigated the Monte-Carlo model to simulate Ag–Au dealloying process, and indicated that dealloying process was confined to the interface region between the alloy and the electrolyte, which was proofed by CHEN-WIEGART et al [4].

Alloys used to dealloying should meet the parting limit, and the mole fraction of the active component should be more than 50% [5]. Precursors were fabricated by melt spin method, laser remelting, electrochemical deposition, and other rapid solidification methods to obtain a single phase and fine microstructure [6–8]. Then, dealloying was carried out by chemical, electrochemical or even melt corrosion method to gain the nanoporous

structure [8–10]. Researchers mainly investigated influence of dealloying parameters, such as electrolyte, corrosion duration, temperature, corrosion current or potential level on dealloyed structures [11–13], and studied the performance and potential application of dealloyed products. They found that dealloyed structures had a very high specific surface area, thus possessed many attractive properties, for example, good catalytic performance, excellent surface-enhanced Raman scattering effect [14–16].

In addition, some researchers focused on the mechanism of dealloying process [1–4], and explained the evolution of porous structure during chemical or electrochemical dealloying process. However, little attention has been paid to the relationship between chemical and electrochemical dealloying, or to the morphology evolution of dealloyed structures under various chemical and electrochemical dealloying conditions.

The author fabricated porous Cu by dealloying the Cu–34.6%Mn (mass fraction) alloy made by the Gasar process. The precursor is a casting alloy with less active component content [17,18], and the dealloyed products are different under various dealloying conditions. In this work, the evolution of nanoporous structures under

different conditions are discussed in the view of diffusion and dissolution, and the relationship between the two dealloying methods is established.

## 2 Experimental

The Gasar Cu–34.6%Mn alloy was prepared by unidirectional solidification with a mould casting process [19]. The obtained Gasar Cu–34.6% Mn alloys were sectioned into samples of slice (8 mm × 8 mm × 0.5 mm) and cuboid (8 mm × 8 mm × 10 mm) and column ( $d3$  mm × 10 mm,  $d10$  mm × 20 mm). After degreasing in acetone, the Gasar samples were polished with 240 grit to 2000 grit SiC papers. Electrochemical dealloying of cuboid samples was carried out in 5% HBF<sub>4</sub> at various current levels ( $2.6 \times 10^3$ – $1.3 \times 10^4$  mA/cm<sup>2</sup>) and durations using a galvanostatic electrochemical cell (DH1765 source) and a stainless steel plate as the cathode [17]. Slices samples were chemically dealloyed under free corrosion at room temperature (0.1 mol/L HCl, 20 °C, 7 d) and elevated temperature (1.2 mol/L HCl, 90 °C, 12 h), respectively. The cuboid and column samples were etched in 1.2 mol/L HCl in a water bath (90 °C) for complete dealloying (32–72 h). After dealloying, the specimens were rinsed with de-ionized water and ethanol to release the residual electrolyte and dried in air freely. The dealloyed morphology and composition were analyzed using a LEO–1530 scanning electron microscopy (SEM) equipped with an INCA X-sight 7573 energy dispersive X-ray spectroscopy (EDS). X-ray diffraction (XRD) patterns were recorded using a D8-Advanced X-ray diffractometer with a Cu K<sub>α</sub> radiation source. The porosity of the hybrid porous structure was detected by an Autopore IV 9510 mercury porosimeter [18].

## 3 Results

To fabricate bulk hybrid porous metals, Gasar Cu–34.6%Mn alloy was dealloyed by electrochemical and chemical corrosion. Four typical dealloyed structures formed under different conditions (Fig. 1). There exist uneven corrosion pits on the surface of samples dealloyed under chemical corrosion at room temperature (Fig. 1(a)), strips with diameters in sub-micrometer scale make up a porous structure inside the corrosion pits (Fig. 1(b)). While dealloying the Gasar Cu–34.6%Mn alloy at elevated temperature (90 °C), a hybrid porous structure was prepared, in which strips with a large aspect ratio stacked uniformly and a nanoporous structure formed throughout the slice sample (Figs. 1(c) and (d)) [18]. So chemical etching enables the formation of a penetrable structure.

By electrochemical dealloying the Gasar Cu–

34.6%Mn alloy at low current level ( $2.6$ – $260$  mA/cm<sup>2</sup>), a haystack porous film generates (Fig. 1(e)) [17]. Whereas a sponge-like porous structure evolves under high current levels ( $2.6 \times 10^3$ – $1.3 \times 10^4$  mA/cm<sup>2</sup>), this porous structure is uniform and bicontinuous (Fig. 1(g)), similar to the traditionally dealloyed structure previously reported [3]. The thickness of the dealloyed structure decreases with increasing current density, which is in the range of dozens of micrometer at low current level (Fig. 1(f)) and sub-micrometer at high current level (Fig. 1(h)), respectively. The compositions of all the four porous structures are Cu-dominated, as detected by EDS spectrum (Table 1).

In addition, bulk hybrid porous metals were prepared by dealloying the slice, cuboid and column Gasar samples in 1.2 mol/L HCl at 90 °C for sufficient time (12–72 h). The colour of samples changed from silvery white to dark red either on the surface or on the fracture, indicating that the samples were dealloyed completely (Fig. 2). High magnification fracture morphology of dealloyed samples is the same as the typical morphology (Fig. 1(c)). The XRD pattern indicates that the precursor is a single-phase solid solution, while Cu is the major phase after dealloying. Thus, a uniform three-dimensional centimeter size scale hybrid porous Cu with a combination of micro–nano double scale pore size and random-regular bimodal is prepared. The dealloyed pore size is mostly in the range of several hundred nanometer size scale, especially 350 nm, analyzed by a mercury porosimetry, and the porosity of the hybrid structure is over 60% [18].

## 4 Discussion

### 4.1 Surface diffusion

Dealloying process is confined to the interface region between the alloy and electrolyte, and dealloying structures originate from the inactive component rearrangement. Thus, the surface diffusion coefficient ( $D_s$ ) of Cu atoms affects the formation of dealloyed structures, and it is necessary to calculate  $D_s$  under different dealloying conditions. QIAN and CHEN [11] studied the dealloying process of Au–Ag binary system and discovered that the inactive component rearrangement was similar to the isothermal grain growth, so that  $D_s$  could be expressed as [20]

$$D_s = D_0 \exp\left(\frac{-E_a}{RT}\right) \quad (1)$$

where  $D_0$  is a pre-exponential factor, for Cu atom,  $D_0 \approx 10^{-4}$  cm<sup>2</sup>/s [21],  $R$  is the gas constant,  $T$  is the corrosion temperature, and  $E_a$  is the activation energy. The value of  $E_a$  at room temperature for free diffusion of Cu atom is about 0.38 eV (36.6 kJ/mol) [22].

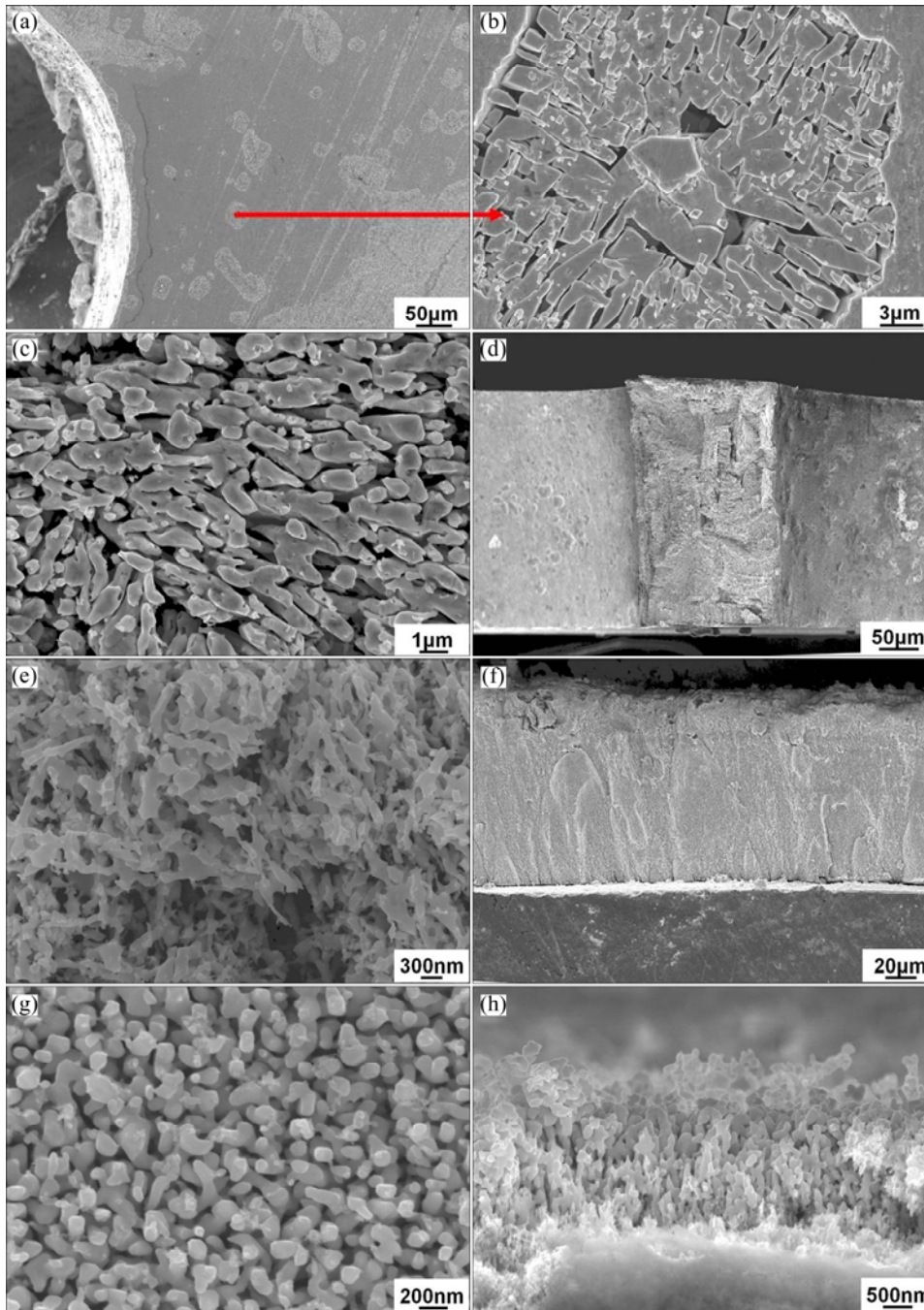


**Fig. 1** Four typical dealloyed structures: (a) and (b) Surface morphology, chemical (0.1 mol/L HCl, 20 °C, 7 d); (c) Surface morphology, chemical (1.2 mol/L HCl, 90 °C, 12 h) [18] and (d) fracture; (e) Surface morphology, electrochemical (5% HBF<sub>4</sub>, 5.2 mA/cm<sup>2</sup>, 5 h) [17] and (f) fracture; (g) Surface morphology, electrochemical (5% HBF<sub>4</sub>, 5.2 × 10<sup>3</sup> mA/cm<sup>2</sup>, 3 min) and (h) fracture

**Table 1** Composition of typical dealloyed structures detected by EDS

Component	Mole fraction/%			
	20 °C, 7 d	90 °C, 12 h	5.2 mA/cm <sup>2</sup> , 5 h	5.2 A/cm <sup>2</sup> , 3 min
Cu	92.4	89.8	92.7	95.9
Mn	4.0	1.7	1.6	4.1
O	3.6	8.5	5.7	0

Neglecting the influence of temperature on  $E_a$ ,  $D_S$  values under different chemical corrosion temperatures are calculated (Table 2). ERLEBACHER [23] presumed that the  $D_S$  of Cu atom under electrochemical corrosion is in the range of  $10^{-10}$  cm<sup>2</sup>/s, and  $D_S$  is enhanced by a factor of order 10 over the potential range of 1 V. Since the critical potential of Cu–38%Mn (mole fraction) is about –150 mV [24], and the voltage of low current level (5.2 mA/cm<sup>2</sup>) dealloying in this work is about 0.8 V, so



**Fig. 2** Gasar Cu–34.6%Mn alloy (silver white), hybrid porous structure (dark red) of different types, and XRD patterns before and after high temperature chemical dealloying [18]

**Table 2** Parameters related to diffusion and dissolution processes

Process	$J/(\text{mA}\cdot\text{cm}^{-2})$	$t/^\circ\text{C}$	$E_a/(\text{kJ}\cdot\text{mol}^{-1})$	$D_S/(\text{cm}^2\cdot\text{s}^{-1})$	$\phi/\text{V}$	$k_D/\text{s}^{-1}$	$k_E/\text{s}^{-1}$	$k_D/k_E$
Chemical dealloying		20	36.6	$3.84\times 10^{-11}$		$3.79\times 10^6$	0.0122	$3.11\times 10^8$
		90	36.6	$5.41\times 10^{-10}$		$5.36\times 10^7$	0.139	$3.86\times 10^8$
Electrochemical dealloying	5.2	20	28.5	$1\times 10^{-9}$	0.4	$9.93\times 10^7$	$5.69\times 10^5$	175
	$5.2\times 10^3$	20	17.1	$1\times 10^{-7}$	0.57	$9.94\times 10^9$	$4.30\times 10^{10}$	0.231

that  $D_S$  of low current level dealloying is in the range of  $10^{-9}$   $\text{cm}^2/\text{s}$ . Besides,  $D_S$  increases linearly with increased current density (Eq. (2)) [25], thus  $D_S$  of high current level ( $5.2\times 10^3$   $\text{mA}/\text{cm}^2$ ) dealloying can be calculated (Table 2). Then, the activation energies  $E_a$  for electrochemical corrosion under different current levels can be calculated (Eq. (1)).

$$D_S = \frac{J_0 N_A x n^2 (2r)^4}{6F} \quad (2)$$

where  $J_0$  is the current density,  $N_A$  is the Avogadro constant,  $x$  is the mole fraction of the base metal atoms in the alloy,  $n$  is the cases where the atom could jump several atomic spaces,  $r$  is the atomic diameter, and  $F$  is the Faraday constant [25].

As can be seen from Table 2,  $D_S$  for 90 °C chemical corrosion and 5.2  $\text{mA}/\text{cm}^2$  electrochemical corrosion are in the same order of magnitude. Since the interface diffusion influences the dealloying process, is it possible to obtain similar dealloyed morphology for the two dealloying processes? Figure 3 shows the high magnitude dealloyed morphology of 90 °C chemical dealloying [18] and 5.2  $\text{mA}/\text{cm}^2$  electrochemical dealloying. The two dealloyed structures are both nanoporous structures, whose strips with a large aspect ratio arrange regularly and make up nanometer pores. Therefore, no matter dealloying is carried out by chemical or electrochemical corrosion, when  $D_S$  is in the same order of magnitude by controlling corrosion parameters, the obtained dealloyed morphology will be similar. While the ligament and pore size of chemical dealloyed structure are larger than those the electrochemical dealloyed structure, due to the

coarsening effect of corrosion time on dealloyed structures (Eq. (3)) [11].

$$d(t) = \left( d_0^4 + \frac{32\gamma a^4 D_S t}{k_B T} \right)^{1/4} \quad (3)$$

where  $t$  is the corrosion time,  $d(t)$  is the pore size of dealloyed structure,  $d_0$  is the initial pore size,  $\gamma$  is the surface energy,  $a$  is the lattice parameter, and  $k_B$  is the Boltzmann constant.

#### 4.2 Competition between diffusion and dissolution

Dealloying process is a competition between the surface roughening and surface smoothing process. But how the two processes transform under different dealloying conditions and bring about the four typical dealloyed structures formation? ERLEBACHER [23] proposed that the dissolution frequency ( $k_E$ ) of active component and the diffusion frequency ( $k_D$ ) of inactive component can be expressed as Eq. (4) and Eq. (5), respectively. Besides,  $k_E$  and  $k_D$  are proportional to the dissolution velocity ( $v_0$ ) and the surface diffusion coefficient ( $D_S$ ), respectively. Thus,  $k_D$  under different dealloying conditions and  $k_E$  of chemical dealloying can be calculated on account of the given data (Table 2).

As for electrochemical dealloying carried out by two electrode source in this work, an equivalent corrosion potential ( $\phi$ ) should be defined firstly, according to the dealloying current and voltage. For electrochemical corrosion at 5.2  $\text{mA}/\text{cm}^2$ ,  $\phi$  can be taken as half of the corrosion voltage (0.8 V). While the dealloying condition of  $5.2\times 10^3$   $\text{mA}/\text{cm}^2$  electrochemical corrosion is much different from the traditional dealloying process, so  $\phi$  should be defined by other

means. The pore size of dealloyed structure is the function of surface diffusion coefficient ( $D_S$ ) and the dissolution velocity ( $v_0$ ) (Eq. (6)) [3], and the pore sizes of low and high current density electrochemical corrosion are 75 nm and 105 nm, respectively. Thus,  $\phi$  of high current density electrochemical corrosion can be calculated with the combination of Eq. (4) and Eq. (6) (Table 2).

$$k_E = v_E \exp[-(E_a - \phi)/(k_B T)] \quad (4)$$

$$k_D = v_D \exp[-E_a / (k_B T)] \quad (5)$$

$$d \propto \left(\frac{D_S}{v_0}\right)^{1/6} \quad (6)$$

where  $v_E$  and  $v_D$  are attempt frequencies,  $v_E=10^4 \text{ s}^{-1}$ ,  $v_D$  is in the order of the Debye frequency ( $v_D=10^{13} \text{ s}^{-1}$ ) [23].  $\phi$  is the equivalent corrosion potential.  $E_a$  is the activation energy,  $d$  is the pore size of dealloyed structure, and  $v_0$  is the dissolution velocity of a flat alloy surface with no copper accumulated on it.

Table 2 indicates that  $k_E$  and  $k_D$  increase with increasing corrosion temperature or corrosion current, both  $k_E$  and  $k_D$  of electrochemical dealloying are larger than those of chemical dealloying. The  $k_D$  of 90 °C chemical corrosion and 5.2 mA/cm<sup>2</sup> electrochemical corrosion are in the same order of magnitude, indicating a similar diffusion velocity of the two processes, and as a result similar dealloying morphology is prepared (Fig. 3).

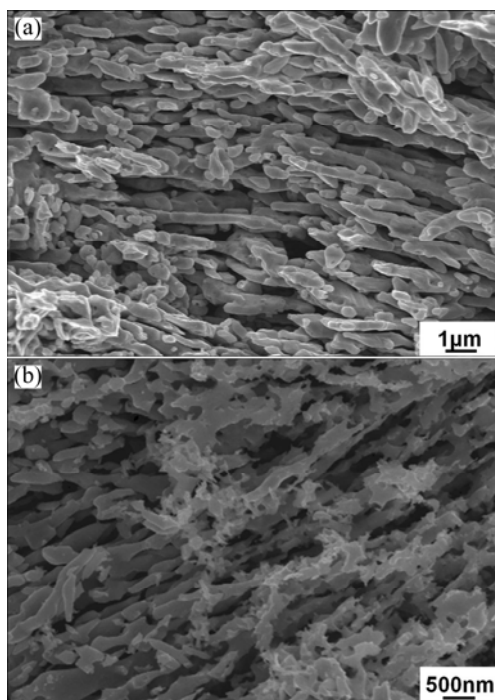


**Fig. 3** Morphologies of nanoporous structure: (a) Chemical (1.2 mol/L HCl, 90 °C, 36 h) [18]; (b) Electrochemical (5% HBF<sub>4</sub>, 2.6 mA/cm<sup>2</sup>, 8 h)

While different kinds of dealloyed structures can be attributed to the change of  $k_D/k_E$  with dealloying parameters. For chemical and low current level electrochemical corrosion (2.6 mA/cm<sup>2</sup>),  $k_D/k_E > 1$ , the surface smoothening process due to the Cu atoms diffusion is prevalent to the surface roughening process due to the Mn atoms dissolution. Mn atoms dissolve gradually and Cu atoms rearrange rapidly, forming porous structure comprising of strips with a large aspect ratio. As for high current level electrochemical corrosion (5.2×10<sup>3</sup> mA/cm<sup>2</sup>),  $k_D/k_E < 1$ , the surface roughening process is prevalent to the surface smoothening process. Mn atoms dissolve faster than Cu atoms diffusion, leading to Cu atoms having less time to rearrange and forming bicontinuous porous structure eventually. So, the surface diffusion coefficient ( $D_S$ ) and the diffusion frequency ( $k_D$ ) of Cu atom, as well as the dissolution frequency ( $k_E$ ) of Mn atom change with dealloying condition, leading to the formation of various dealloyed morphologies and structures.

## 5 Conclusions

1) Four typical dealloyed structures are fabricated by dealloying the Gasar Cu–34.6%Mn alloy under various conditions, and a centimeter size scale hybrid porous metal is prepared by dealloying the column Gasar sample in 1.2 mol/L HCl at 90 °C for 72 h.

2) When the surface diffusion coefficient ( $D_S$ ) of Cu atom is in the same order of magnitude, the dealloyed morphology is identical either by chemical or electrochemical corrosion, with large aspect ratio strips making up nanometer pores.

3) The dissolution frequency ( $k_E$ ) and the diffusion frequency ( $k_D$ ) increase with increasing corrosion temperature or corrosion current.

4) For chemical and low current level electrochemical corrosion (5.2 mA/cm<sup>2</sup>),  $k_D/k_E > 1$ , the surface smoothening process due to Cu atoms diffusion is prevalent to the surface roughening process due to Mn atoms dissolution, Cu atoms rearrange rapidly and form strips with a large aspect ratio. As for high current level electrochemical corrosion (5.2×10<sup>3</sup> mA/cm<sup>2</sup>),  $k_D/k_E < 1$ , the surface roughening process is prevalent to the surface smoothening process, Mn atoms dissolve quickly, Cu atoms have less time to rearrange and form bicontinuous porous structure eventually.

## References

- [1] STRATMANN M, ROHWERDER M. Materials science—A pore view of corrosion [J]. Nature, 2001, 410(6827): 420–423.
- [2] NEWMAN R C, CORCORAN S G, ERLEBACHER J, AZIZI M J, SIERADZKI K. Alloy corrosion [J]. MRS Bulletin, 1999, 24(7): 24–28.

- [3] ERLEBACHER J, AZIZ M J, KARMA A, DIMITROV N, SIERADZKI K. Evolution of nanoporosity in dealloying [J]. Nature, 2001, 410(6827): 450–453.
- [4] CHEM-WIEGART Y C K, WANG S, LEE W K, MCNULTY I, VOORHEES P W, DUNAND D C. In situ imaging of dealloying during nanoporous gold formation by transmission X-ray microscopy [J]. Acta Materialia, 2013, 61(4): 1118–1125.
- [5] SCHOFIELD E. Anodic routes to nanoporous materials [J]. Transactions of the Institute of Metal Finishing, 2005, 83(1): 35–42.
- [6] ZHANG Zhong-hua, WANG Yan, QI Zhen, ZHAHANG Wen-hua, QIN Jing-yu, FRENZEL J. Generalized fabrication of nanoporous metals (Au, Pd, Pt, Ag, and Cu) through chemical dealloying [J]. Journal of Physical Chemistry C, 2009, 113(29): 12629–12636.
- [7] DONG Chang-sheng, GU Yu, ZHONG Min-lin, LI Lin, SEZER K, MA Ming-xing, LIU Wen-jin. Fabrication of superhydrophobic Cu surfaces with tunable regular micro and random nano-scale structures by hybrid laser texture and chemical etching [J]. Journal of Materials Processing Technology, 2011, 211(7): 1234–1240.
- [8] HAYES J R, HODGE A M, BIENER J, HAMZA A V, SIERADZKI K. Monolithic nanoporous copper by dealloying Mn–Cu [J]. Journal of Materials Research, 2006, 21(10): 2611–2616.
- [9] LIN Y W, TAI C C, SUN I W. Electrochemical preparation of porous copper surfaces in zinc chloride-1-ethyl-3-methyl imidazolium chloride ionic liquid [J]. Journal of the Electrochemical Society, 2007, 154(6): D316–D321.
- [10] WADA T, YBUTA K, INOUE A, KATO H. Dealloying by metallic melt [J]. Materials Letters, 2011, 65(7): 1076–1078.
- [11] QIAN L H, CHEN M W. Ultrafine nanoporous gold by low-temperature dealloying and kinetics of nanopore formation [J]. Applied Physics Letters, 2007, 91: 083105.
- [12] XU Jun-ling, WANG Yan, ZHANG Zhong-hua. Potential and concentration dependent electrochemical dealloying of Al<sub>2</sub>Au in sodium chloride solutions [J]. Journal of Physical Chemistry C, 2012, 116: 5689–5699.
- [13] DONG Chang-sheng, ZHONG Min-lin, HUANG Ting, MA Ming-xing, WORTMANN D, BRAJDIC M, KELBASSA I. Photodegradation of methyl orange under visible light by micro-nano hierarchical Cu<sub>2</sub>O structure fabricated by hybrid laser processing and chemical dealloying [J]. ACS Applied Materials Interfaces, 2011, 3(11): 4332–4338.
- [14] BIENER J, HODGE A M, HAYES J R, VOLKERT C A, ZEPEDA-RUIZ L A, HAMZA A V, ABRAHAM F F. Size effects on the mechanical behavior of nanoporous Au [J]. Nano Letters, 2006, 6(10): 2379–2382.
- [15] ZHANG L, CHEN L Y, LIU H W, HOU Y, HIRATA A, FUJITA T, CHEN M W. Effect of residual silver on surface-enhanced Raman scattering of dealloyed nanoporous gold [J]. Journal of Physical Chemistry C, 2011, 115(40): 19583–19587.
- [16] DING Y, CHEN M W. Nanoporous metals for catalytic and optical applications [J]. MRS Bulletin, 2009, 34(8): 569–576.
- [17] ZHANG Xing-ming, LI Yan-xiang, LIU Yuan, ZHANG Hua-wei. Fabrication of a bimodal micro/nanoporous metal by the Gasar and dealloying processes [J]. Materials Letters, 2013, 92(3): 448–451.
- [18] ZHANG Xing-ming, LI Yan-xiang, ZHANG Hua-wei, LIU Yuan. Fabrication of a three-dimensional bimodal porous metal [J]. Materials Letters, 2013, 106: 417–420.
- [19] JIANG Guang-rui, LI Yan-xiang, LIU Yuan. Influence of solidification mode on pore structure of directionally solidified porous Cu–Mn alloy [J]. The Chinese Journal of Nonferrous Metals, 2011, 21(1): 88–95. (in Chinese)
- [20] BURKE J E. Some factors affecting rate of grain growth in metals [J]. American Institute of Mining and Metallurgical Engineers, 1949, 185(11): 881–886.
- [21] WANG Y X, PANZ Y, LIU T J, JIANG X M, ZHOU L, ZHU J. Anisotropic diffusion of Cu adatoms on strained Cu (111) surface [J]. Applied Surface Science, 2006, 253(4): 1748–1752.
- [22] SHIANG K D. Theoretical studies of atom diffusion on metal surfaces [J]. Physics Letters A, 1993, 180(6): 444–452.
- [23] ERLEBACHER J. An atomistic description of dealloying-porosity evolution, the critical potential, and rate-limiting behavior [J]. Journal of the Electrochemical Society, 2004, 151(104): C614–C626.
- [24] KAN Yi-de. Research on preparation of mesoporous coatings by laser cladding [M]. Beijing: Tsinghua University, 2008. (in Chinese)
- [25] GALVELE J, DUFFO G. Calculation of the surface self-diffusion coefficient,  $D_s$ , induced by the exchange current density,  $i_0$ , application to stress corrosion cracking [J]. Corrosion Science, 1997, 39(3): 605–608.

## Gasar Cu–Mn 合金脱合金腐蚀的组织演变

张星明<sup>1</sup>, 李言祥<sup>1,2</sup>, 张华伟<sup>1,2</sup>, 刘源<sup>1,2</sup>

1. 清华大学 材料学院, 北京 100084

2. 清华大学 先进成形制造教育部重点实验室, 北京 100084

**摘要:** 研究了不同腐蚀条件下, Gasar Cu–34.6%Mn 合金经脱合金腐蚀后的腐蚀形貌变化, 揭示了脱合金组织的形成机理。通过对 Gasar Cu–34.6%Mn 合金进行低温化学腐蚀、高温化学腐蚀、低电流以及高电流电化学腐蚀, 分别制备得到了不均匀的腐蚀凹坑、复合多级孔组织、草垛状结构以及双连续多孔组织 4 种典型的腐蚀组织。为研究不同脱合金组织的形成机制, 计算不同实验条件下 Cu 原子表面扩散系数( $D_s$ )、扩散频率( $k_D$ )以及 Mn 原子的溶解频率( $k_E$ )。研究发现, 化学腐蚀和低电流电化学腐蚀因具有相近的  $D_s$  而具有相近的腐蚀形貌。此外, 随着  $k_D/k_E$  的减小, 脱合金组织由复合多级孔组织转变为双连续多孔薄膜。

**关键词:** Gasar 工艺; 脱合金; 复合多级孔; 纳米多孔组织

(Edited by Yun-bin HE)